

1-1-2010

Dynamic line-by-line pulse shaping with GHz update rate

M. Akbulut
University of Central Florida

S. Bhooplapur
University of Central Florida

I. Ozdur
University of Central Florida

J. Davila-Rodriquez
University of Central Florida

P. J. Delfyett
University of Central Florida

Find similar works at: <https://stars.library.ucf.edu/facultybib2010>

University of Central Florida Libraries <http://library.ucf.edu>

This Article is brought to you for free and open access by the Faculty Bibliography at STARS. It has been accepted for inclusion in Faculty Bibliography 2010s by an authorized administrator of STARS. For more information, please contact STARS@ucf.edu.

Recommended Citation

Akbulut, M.; Bhooplapur, S.; Ozdur, I.; Davila-Rodriquez, J.; and Delfyett, P. J., "Dynamic line-by-line pulse shaping with GHz update rate" (2010). *Faculty Bibliography 2010s*. 6934.
<https://stars.library.ucf.edu/facultybib2010/6934>

Dynamic line-by-line pulse shaping with GHz update rate

M. Akbulut,^{1,2} S. Bhooplapur,¹ I. Ozdur,¹ J. Davila-Rodriguez,¹ and P. J. Delfyett^{1*}

¹ CREOL: The College of Optics and Photonics, University of Central Florida, Orlando, FL 32816, USA

² current address: Fibertek Inc., Herndon, VA 20170, USA

*delfyett@creol.ucf.edu

Abstract: We introduce a novel scheme for dynamic line-by-line pulse shaping with GHz update rates. Four lines of an optical frequency comb source are used to injection-lock four individual VCSEL, which are subsequently electrically modulated at 0.4 to 1GHz through current modulation. This concept could be considered a completely new way of pulse shaping as the light is not simply modified, but rather regenerated with the desired properties. We also discuss an important drawback of line-by-line pulse shapers that ultimately limits the modulation speed capability.

©2010 Optical Society of America

OCIS codes: (320.5540) Pulse shaping; (140.7090) Ultrafast Lasers; (140.3520) Lasers, injection-locked

References and links

1. Z. Jiang, C. Huang, D. E. Leaird, and A. M. Weiner, "Optical arbitrary waveform processing of more than 100 spectral comb lines," *Nat. Photonics* **1**(8), 463–467 (2007).
2. N. K. Fontaine, R. P. Scott, J. Cao, A. Karalar, W. Jiang, K. Okamoto, J. P. Heritage, B. H. Kolner, and S. J. B. Yoo, "32 Phase X 32 amplitude optical arbitrary waveform generation," *Opt. Lett.* **32**(7), 865–867 (2007).
3. M. J. R. Heck, P. Munoz, B. W. Tilma, E. A. J. M. Bente, Y. Barbarin, O. Yok-Siang, R. Notzel, and M. K. Smit, "Design, Fabrication and Characterization of an InP-Based Tunable Integrated Optical Pulse Shaper," *IEEE J. Quantum Electron.* **44**(4), 370–377 (2008).
4. W. Jiang, F. M. Soares, S. Seo, J. H. Baek, N. K. Fontaine, R. G. Broeke, J. Cao, J. Yan, K. Okamoto, F. Olsson, S. Lourduoss, A. Pham, and S. J. B. Yoo, "A Monolithic InP-Based Photonic Integrated Circuit for Optical Arbitrary Waveform Generation," in *National Fiber Optic Engineers Conference*, OSA Technical Digest (CD) (Optical Society of America, 2008), paper JThA39.
5. F. M. Soares, J. H. Baek, N. K. Fontaine, X. Zhou, Y. Wang, R. P. Scott, J. P. Heritage, C. Junesand, S. Lourduoss, K. Y. Liou, R. A. Hamm, W. Wang, B. Patel, S. Vatanapradit, L. A. Gruezeke, W. T. Tsang, and S. J. B. Yoo, "Monolithically Integrated InP Wafer-Scale 100-Channel \times 10-GHz AWG and Michelson Interferometers for 1-THz-Bandwidth Optical Arbitrary Waveform Generation," in *Optical Fiber Communication Conference*, OSA Technical Digest (CD) (Optical Society of America, 2010), Paper OThS1.
6. N. Hoghooghi, I. Ozdur, M. Akbulut, J. Davila-Rodriguez, and P. J. Delfyett, "Resonant cavity linear interferometric intensity modulator," *Opt. Lett.* **35**(8), 1218–1220 (2010).
7. I. Ozdur, M. Akbulut, N. Hoghooghi, D. Mandridis, S. Ozharar, F. Quinlan, and P. J. Delfyett, "A Semiconductor-Based 10-GHz Optical Comb Source With Sub 3-fs Shot-Noise-Limited Timing Jitter and 500-Hz Comb Linewidth," *IEEE Photon. Technol. Lett.* **22**(6), 431–433 (2010).
8. V. R. Supradeepa, C. B. Huang, D. E. Leaird, and A. M. Weiner, "Femtosecond pulse shaping in two dimensions: towards higher complexity optical waveforms," *Opt. Express* **16**(16), 11878–11887 (2008).
9. Princeton Optronics, "8x8 Addressable VCSEL Array datasheet," <http://www.princetonoptronics.com/pdfs/AA64-BC-SM-W0975.pdf>
10. C. Chang, L. Chrostowski, and C. J. Chang-Hasnain, "Injection-locking of VCSELs," *IEEE J. Sel. Top. Quantum Electron.* **9**(5), 1386–1393 (2003).
11. J. T. Willits, A. M. Weiner, and S. T. Cundiff, "Theory of rapid-update line-by-line pulse shaping," *Opt. Express* **16**(1), 315–327 (2008).
12. D. J. Geisler, N. K. Fontaine, T. He, R. P. Scott, L. Paraschis, J. P. Heritage, and S. J. B. Yoo, "Modulation-format agile, reconfigurable Tb/s transmitter based on optical arbitrary waveform generation," *Opt. Express* **17**(18), 15911–15925 (2009).

1. Introduction

Ability to generate large-bandwidth, arbitrarily-shaped waveforms in optical and microwave domains serve many applications, among which are bandwidth-efficient telecommunications, parallel signal processing and pattern recognition, remote sensing, and physical sciences. To date, the most mature and versatile way to generate large-bandwidth arbitrary waveforms is through line-by-line ultrafast optical pulse shaping [1]. In this technique, an arbitrary, complex optical filter function $H(\omega)$ is designed and applied to individual lines or groups of lines of a optical frequency comb source in order to yield the desired waveform in time-domain. A variety of periodic arbitrary waveforms have been generated with line-by-line pulse shapers based on liquid-crystal based spatial light modulators [1] and resistive-heating of waveguides [2]. Nevertheless these techniques are limited to ~kHz update rates which restricts their use. Recently, fast dynamic pulse shaping schemes based on hybrid, on-chip electro-optic waveguides were shown [3–5]. However, these schemes suffer from practical limitations in scalability due to increasing complexity of fabrication and electrical/optical cross-connects as the number of comb lines, hence the waveform bandwidth, increase.

In this paper, we introduce a novel scheme for line-by-line pulse shaping with GHz update rates, and straight forward scalability to large number of lines. The concept is based on injection-locking of semiconductor lasers. The individual lines of a frequency comb source are used to injection-lock individual Vertical Cavity Surface Emitting Lasers (VCSELs). The VCSELs subsequently are current-injection-modulated in order to regenerate the lines of the frequency comb with the desired amplitude and phase functions. In fact, this concept could be considered a completely new type of pulse shaping, where the source light is not simply modified, but rather regenerated with the desired properties. Owing to the large current-modulation bandwidth of VCSELs, potentially tens of GHz update rates could be achieved.

We experimentally show line-by-line pulse shaping through injection-locking of 4 individual VCSELs with a frequency comb source with 12.5 GHz repetition rate. Each regenerated line was sine-wave modulated at 0.4 to 1 GHz, generating an arbitrary optical waveform with a 5 ns period and 37.5 GHz bandwidth. The modulation speed was mainly limited by the passband of the dispersive optical element in the line-by-line pulse shaper. We believe that this limitation is one of the biggest hurdles in increasing the modulation speed of any continuous spectral-dispersion based arbitrary waveform generation architecture.

2. Injection-Locking concept and experimental results

Injection-locking is commonly used to generate coherent laser sources that share a phase relationship. When a free-running slave laser cavity is injected with the light from a master laser, the slave cavity locks its frequency to the master laser. Moreover, the relative phase of the slave laser obeys Adler's equation (for small injection):

$$\phi = \arcsin\left(\frac{\omega_s - \omega_m}{B}\right) \quad (1)$$

where ϕ is the optical phase difference of the slave and master lasers, ω_s and ω_m are free-running slave and master laser frequencies, and B is the half locking bandwidth. It is evident from Eq. (1) that, once the injection-locking occurs, any perturbation of the slave cavity will result in a relative phase change. Especially for semiconductor lasers, this perturbation could be through current-injection, which in turn yields a high-speed, intrinsically nonlinear phase modulator with applications in optical sampling and telecommunications [6].

Normally, bias current is utilized to tune the frequency of semiconductor lasers at high speeds. However, as the injection-locking process fixes the frequency (defined by the master laser), the bias current ends up tuning the optical phase. The phase of an injection-locked semiconductor laser can be tuned for a full π through the bias current. The bias current range for this tuning is called as – referred by the free-running slave laser frequency change- the

injection-locking bandwidth. Injection-locking bandwidth depends on the master/slave optical injection power ratio. Additionally, the response speed of the phase tuning process goes from DC to a few tens of GHz based on the semiconductor device structure and electrical connections. We have previously demonstrated such operation of a VCSEL up to a few GHz as shown in [6]. Since the VCSEL cavities are very sensitive to bias current, the full π phase swing can be achieved with a very small bias current range, without any significant additional amplitude modulation. Obviously, this requires a very small master/slave optical injection power ratio (usually below -25 dB). If necessary, stronger bias current modulation can be achieved (without the slave laser falling out of injection-lock) by increasing the master laser optical injection power. However, this results in additional direct intensity modulation of the slave laser output along with the phase modulation from the injection-locking process. In this paper, we utilize these high-speed phase and intensity modulation schemes for dynamic line-by-line pulse shaping.

The pulse-shaper setup is shown in Fig. 1. A 1538nm single-frequency laser was modulated with a 12.5 GHz sine-wave by cascaded electro-optic intensity modulators in order to generate a frequency comb source with ~ 5 comb lines of equal power (Fig. 1). Alternatively, a frequency-stabilized 12.5 GHz repetition-rate modelocked laser could be used as the source [7]. The signal was then amplified and fed into a fiber-pigtailed Virtually-Imaged Phase Array (VIPA) based spectral demultiplexer with 6.25 GHz channel separation and 100 GHz free spectral range. Four odd channel outputs of the demultiplexer (frequency separation of 12.5 GHz each) were connected to 4 individual commercial fiber-pigtailed single-mode VCSELs at ~ 1538 nm center wavelength. No effort was spent on actively stabilizing VCSEL temperatures, fiber lengths and polarization fluctuations. The VCSELs were tuned with DC-current to fall within the locking bandwidth of the corresponding injecting comb line, and directly-modulated with various RF power levels at 0.4GHz, 0.6GHz, 0.8GHz, and 1GHz with sine-wave generators that share a common reference clock. The peak-to-peak optical intensity modulation depth of the VCSELs ranged from 2% to 20% with various RF power levels, and the optical injection ratio varied from -23 dB to -17 dB. The VCSEL optical outputs were isolated from the input demultiplexer with circulators in order to prevent the reflections from flat fiber tips that could destabilize the injection-locking process. An output spectral multiplexer that is identical to the input demultiplexer was used in the VCSEL output signal path to observe the resultant shaped arbitrary waveforms. The waveforms were characterized with a high-resolution Optical Spectrum Analyzer (OSA), Radio Frequency (RF) spectrum analyzer, a sampling oscilloscope and two different speed real-time oscilloscopes. Although simple sine-wave modulation was implemented here as a proof-of-principle, work is ongoing with complex modulation waveforms involving high-speed bit pattern generators.

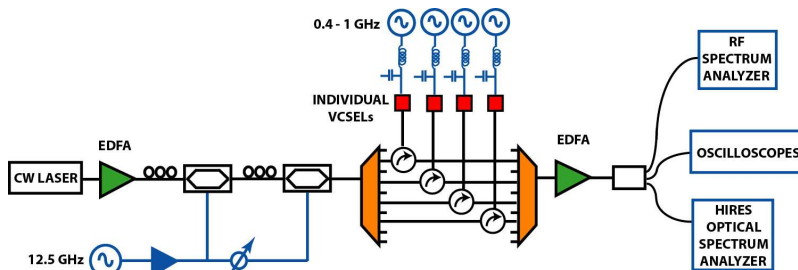


Fig. 1. Experiment Setup for GHz Update Rate Line-by-Line Pulse Shaping

The measured high resolution optical spectra and RF spectra are shown in Fig. 2 with and without injection-locking for -25 dBm, -30 dBm, and -35 dBm RF modulation powers. It can be easily seen from the RF traces that there was no phase relationship between free-running VCSELs before injection-locking, however injection-locked traces show clear tones with high

Signal to Noise Ratio (SNR). Furthermore, the high resolution optical spectrum trace confirms that the linewidths of the VCSELs were narrowed by injection-locking as expected.

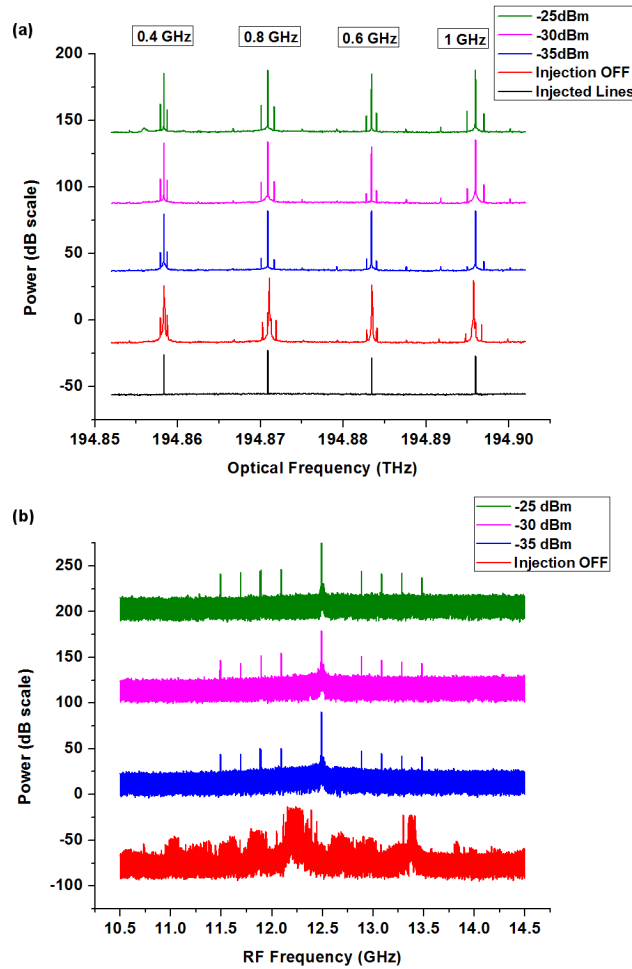


Fig. 2. (a) High Resolution Optical Spectra, and (b) RF Spectra. Both shown with and without injection-locking for various RF modulation power levels.

Initially, we tried to observe the time-domain waveform with a high-speed sampling oscilloscope. Although certain periodicity of the generated waveform could be seen on the sampling scope traces, clear waveforms could not be observed due to the slow triggering speed of the scope relative to the environmental fluctuations of the VCSEL pigtail fibers. The time-domain data from a two different speed real-time oscilloscopes are shown in Fig. 3 for -25dBm and -30dBm RF modulation power levels. A 1GHz , 5Gs/s real-time oscilloscope was used to obtain the overall time envelope data, which was subsequently Fourier-transformed to yield clean RF frequencies with $>30\text{dB}$ SNR (Fig. 3(d)) confirming the RF spectrum analyzer measurement of Fig. 2. Additionally, a 16GHz , 40Gs/s real-time oscilloscope (LeCroy WaveMaster 816zi) was utilized to observe a periodic arbitrary waveform with 5ns period, which corresponds to the lowest common multiple of the individual VCSEL modulation periods (Fig. 3(a)). Again, the noise in the time-domain trace is attributed to the environmental fluctuations of the VCSEL pigtail fibers causing fast phase and polarization fluctuations. Nevertheless, subsequent Fourier-transform of the data yields clean RF frequencies at $0.4, 0.6, 0.8, 1\text{ GHz}$, and $12.5 \pm 0.4, 0.6, 0.8, 1\text{ GHz}$ (Fig. 3(b)). Moreover,

intermixing products and higher order RF beats are also observed up to 20 GHz, limited by the 10 GHz photodetector and 16 GHz oscilloscope bandwidth. A sample simulation of the system is also shown in Fig. 3(c). that is qualitatively similar the observed waveform. We believe that the stronger portion of the modulation was due to the direct intensity modulation of the lines with moderate modulation depth, while some portion came from the phase modulation. In fact, injection-locking bandwidth, intensity modulation bandwidth, and phase modulation depth are all functions of the power injection ratio, and we are working on identifying these parameters in order to calibrate and model our system more accurately.

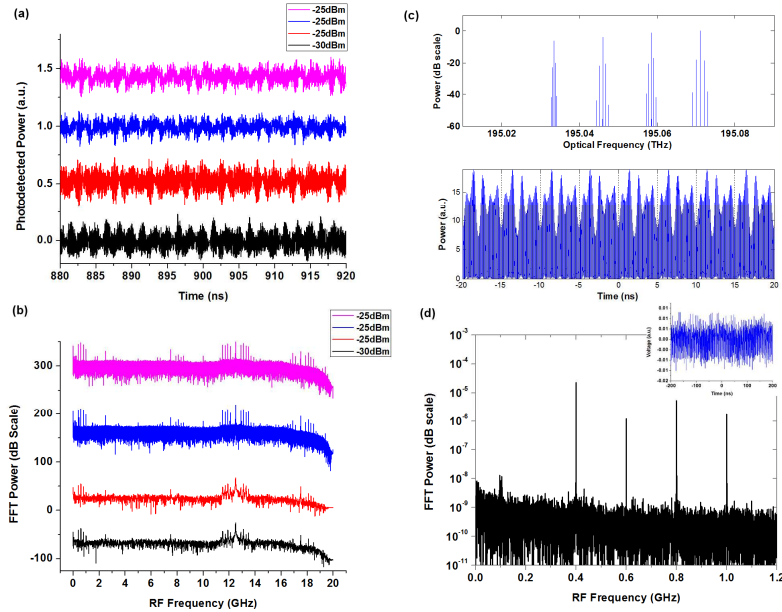


Fig. 3. (a) 16GHz real-time scope traces, (b) Corresponding Fourier-transforms, (c) Sample simulation, (d) Fourier-transform of 1GHz real-time scope trace (inset).

3. Discussion

In this work, we used direct current-modulation of the VCSELs to achieve intensity and phase modulation. Additionally, one can carefully modulate the VCSELs with a very small depth as to achieve phase-only modulation as in [6]. Furthermore, combination of a portion of the original master signal with the injection-locked phase-only modulated slave signal can yield precisely controlled intensity and phase modulation.

Another, more preferred implementation of our pulse shaping scheme can be realized with a 1-Dimensional free space VCSEL array. This would eliminate the non-common fiber pigtail paths and improve the long term stability. However, in this case, alignment of the pulse shaper becomes more challenging due to the increased number of dimensions. Namely, every source frequency line should overlap with the individual VCSEL frequency injection-locking band, and individual VCSEL spatial location. Besides the alignment challenges, this implementation allows straightforward scaling of the number of VCSELs, especially via 2-Dimensional VCSEL arrays and 2-Dimensional pulse shaping [8]. Fabrication and electrical cross-connect wiring of 2-Dimensional VCSEL arrays are well-established techniques in the industry [9]. One advantage of the two dimensions is that scaling from a single channel to N channels requires a maximum of $N^{1/2}$ increase in the physical dimensions of the system, therefore enabling scaling to hundreds of channels with minimized engineering challenges.

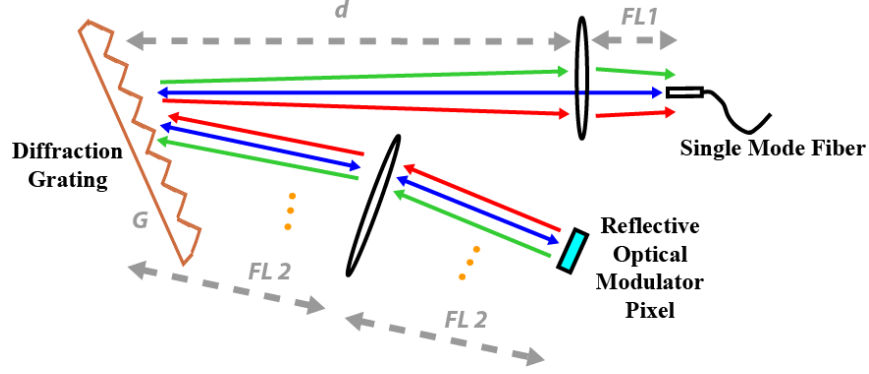


Fig. 4. Regular Reflective Diffraction Grating Based Pulse Shaper - Only one modulated Frequency Line is shown.

It is evident in Fig. 2 and Fig. 3 that, as the modulation frequency was increased, the sideband power ratio diminished in the dynamic pulse shaper. This evidence points to an upper limitation of the modulation frequency of the optical comb lines. The commercial VCSELs used in the experiment had a free-running rise time of ~ 100 ps, and the injection-locking process is expected to reduce the rise time even more to reach tens of GHz modulation bandwidth [10]. Thus, the main limitation of the upper modulation frequency of the optical comb lines is not the VCSELs, but rather the spectral multiplexer. In order to explain this, let's assume a standard, reflective, "zero-dispersion 4-f" diffraction grating based line-by-line pulse shaper setup (Fig. 4). The pulse shaper includes two lenses for imaging the input light to the plane of the optical modulator array. In Fig. 4, for simplicity, only a single modulator pixel is shown corresponding to a single optical frequency comb line. The grating equation for a single comb line at the optical frequency of ν_0 can be written as (Eq. (2)):

$$\theta_m = \arcsin\left(\frac{cG}{\nu_0} - \sin(\theta_d)\right) \quad (2)$$

where c is the speed of light, G is the groove density, θ_m is the input angle of the beam, and θ_d is the diffraction angle of the comb line of interest. The individual pixels of the spatial light modulator in a regular "static" pulse shaper are passive, and do not change the optical frequencies - they just introduce a static optical phase. However, in the case of active VCSELs along with modulation, new frequencies are generated. For a VCSEL injection-locking to the input optical frequency of ν_0 , a simple small-signal sine-wave modulation at f_m generates the frequency components " $\nu_0 - f_m$ " and " $\nu_0 + f_m$ ". The intensities of these components will depend on the strengths of phase modulation and intensity modulation of the VCSEL. The problem arises from the fact that, these new frequencies are emitted by the same VCSEL aperture that regenerates the original ν_0 signal. Therefore, on the return path, the diffraction grating directs " $\nu_0 - f_m$ " and " $\nu_0 + f_m$ " at slightly different angles (θ_- and θ_+) compared to ν_0 . Consequently, the newly generated frequencies do not couple back into the pulse shaper input aperture with the same efficiency as ν_0 . The angles θ_- and θ_+ are given by Eq. (3):

$$\begin{aligned} \theta_- &= \arcsin\left(\frac{cG}{(\nu_0 - f_m)} - \sin(\theta_d)\right) \\ \theta_+ &= \arcsin\left(\frac{cG}{(\nu_0 + f_m)} - \sin(\theta_d)\right) \end{aligned} \quad (3)$$

If we assume a thin-lens with focal length FL_1 at distance d , a single mode fiber with core diameter $2a$ as the aperture, and perfect coupling of the ν_0 component back into the single

mode fiber, the power coupling ratio of the new frequencies can be simply estimated in dB-scale, shown below as P_- and P_+ . Here, we show simplified analytical derivations of the phenomena, while a more generalized and detailed study can be found in [11]. We assume a flat beam profile for simplicity of the analytical derivation, however this can easily be extended to a Gaussian beam profile by the use of “Error Function” in the overlap integral calculations. In fact, the flat beam profile assumption gives a rather optimistic estimate of the coupling efficiencies compared to a Gaussian beam profile. Additionally, the numerical aperture (NA) of the single mode fiber is not considered due to the difference between (θ_- and θ_+) and θ_{in} being much smaller than the NA for practical implementations.

$$\begin{aligned}
 P_- &= 10 \log_{10} \left(\frac{1}{2} + \frac{1}{2 \cos \left(\left\{ 1 - \frac{d}{FL_1} \right\} \times \{ \theta_- - \theta_{in} \} \right)} - \left(\frac{FL_1 \tan[\theta_- - \theta_{in}]}{2a} \right) \right) \\
 P_+ &= 10 \log_{10} \left(\frac{1}{2} + \frac{1}{2 \cos \left(\left\{ 1 - \frac{d}{FL_1} \right\} \times \{ \theta_{in} - \theta_+ \} \right)} - \left(\frac{FL_1 \tan[\theta_{in} - \theta_+]}{2a} \right) \right)
 \end{aligned} \tag{4}$$

It can be seen from Eq. (4) that, the modulation depth is reduced for the center line frequency ν_0 due to the non optimal spectral multiplexing. In fact, for a 3-dB reduction and total cutoff of the new frequency components, the maximum modulation frequencies can be calculated as (the cosine term in the denominator ≈ 1):

$$\begin{aligned}
 f_{m-3dB} &= \pm \left(\nu_0 - \frac{cG}{\sin \left[\theta_{in} + \arctan \left(\frac{a}{FL_1} \right) \right] + \sin(\theta_d)} \right) \\
 f_{m-cutoff} &= \pm \left(\nu_0 - \frac{cG}{\sin \left[\theta_{in} + \arctan \left(\frac{2a}{FL_1} \right) \right] + \sin(\theta_d)} \right)
 \end{aligned} \tag{5}$$

A plot showing the power coupling ratio for practical numbers of $\nu_0 = 193.55$ THz (1550 nm wavelength), $G = 1200$ lines/mm, $\theta_{in} = 72.5^\circ$, $a = 5\mu\text{m}$, $d = 20\text{cm}$ and two cases of $FL_1 = 4\text{cm}$ and $FL_1 = 20\text{cm}$ is displayed in Fig. 5. For a given focal length FL_1 , the power coupling ratio for the positive and negative sidebands are essentially equal as seen by overlapping lines in Fig. 5. The 3-dB modulation frequencies are calculated from Eq. (5) as ~ 3.91 GHz and ~ 0.78 GHz for 4 cm and 20 cm focal lengths respectively. Almost no optical power couples back into the fiber for modulation frequencies beyond ~ 7.82 GHz and ~ 1.56 GHz for each case. Although the modulation speed is increased for smaller values of FL_1 , it should be noted that the spectral resolution (thus the generated waveform fidelity) of the pulse shaper is directly proportional to FL_1 [1]. Consequently, there is a tradeoff between dynamic line-by-line modulation speed and waveform fidelity.

Similar equations can be derived for continuously dispersing VIPA and Arrayed Waveguide Grating (AWG) based pulse shapers. We believe this simple mechanism will be

the fundamental speed limitation of any pulse shaper that utilizes a continuous spectral-disperser and high speed line-by-line modulation.

Recently, new AWG designs yielding raised cosine filter functions were proposed for line-by-line pulse shaping [12]. These AWGs are optimized for fixed discrete channels, and the filter function of each channel has a large overlap with adjacent channels. For standard high speed line-by-line modulation, these overlaps would cause crosstalk between channels, and limit modulation speed in a similar fashion as above. In order to avoid the crosstalk, more complicated modulation schemes such as I/Q modulation and pre-emphasis are required. Although this combination alleviates the problem, it increases the system complexity and cost, therefore we believe that it is not the best solution.

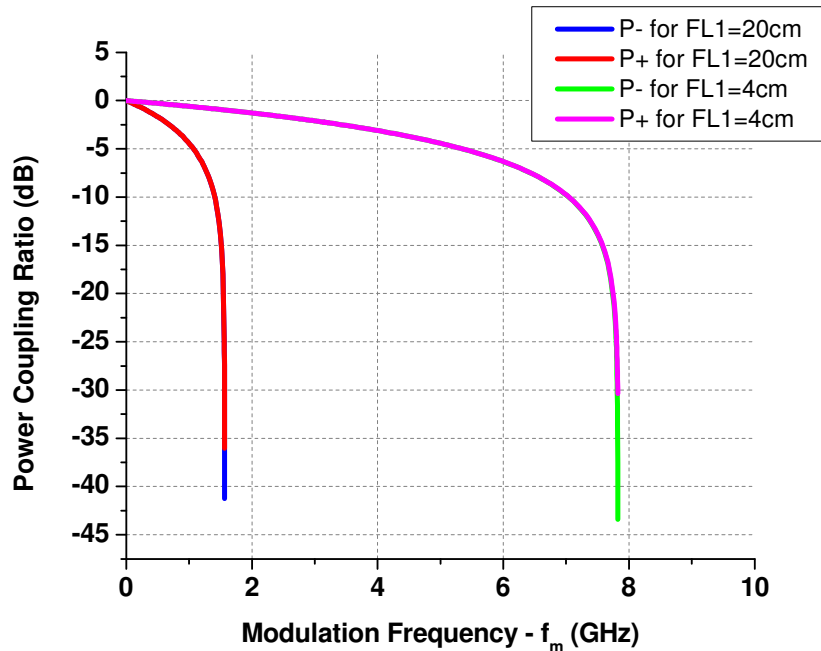


Fig. 5. Power Coupling Ratio into Input Aperture vs. Modulation Frequency for Uniform Beam Shape.

4. Conclusion

In conclusion, we have introduced a novel line-by-line pulse shaping scheme that enables potentially tens of GHz update rates with straight forward scalability for channel count. We have experimentally shown 4 individual lines sine-wave modulated at 0.4 to 1 GHz, generating an arbitrary waveform with a 5 ns period and 37.5 GHz bandwidth. We also discuss a simple fundamental mechanism that ultimately limits the modulation speed capability of any line-by-line pulse shaper that is based on continuous spectral dispersion.

Acknowledgments

The authors would like to thank Robert Hanson of LeCroy Corp. for the loan of LeCroy WaveMaster 816zi real-time oscilloscope.